Research on Anti-freezing Method of Aircraft Water System Pipelines

Yan Ma

Shanghai Aircraft Design and Research Institute, Shanghai, 201210, China

mayan@comac.cc

Abstract. When aircrafts operate in cold regions, electric heat tracing is usually used to heat the water system pipelines to avoid icing. Based on aircrafts operational scenarios, this article analyzed the enclosed and semi-open compartment environments and the heat loss laws of pipelines, determining the power of electric heat tracing. Using MATLAB PDE-tool, the temperature distributions of pipelines with electric heat tracing were solved. The results indicated that the power of electric heat tracing worked well to maintain the water temperature within the target temperature range, providing a theoretical basis for the anti-freezing design of aircraft water system pipelines.

Keywords: water system pipelines, anti-freezing, electric heat tracing, PDE-tool

1 Instruction

The water system is used to store and provide sufficient water for the aircrafts, pressurizing water to galleys and lavatories onboard for drinking, washing and toilets flushing, meeting the physiological needs of passengers onboard [1-2]. According to the experience of airlines, during winter, especially when operating in cold regions, the water system should be immediately pressurized to discharge after landing [3]. Because water system pipelines are usually installed below the cabin floor and are often close to the aircraft skin, there is still a need for anti-icing in cold regions. At present, there are two common ways to prevent pipelines icing: electric heat tracing and water heat tracing [4]. Due to the limited space on the aircraft, electric heat tracing has become the preferred choice because of its uniform heating, small layouts and good maintainability.

The water system shall function fully within the whole flight envelope. When determining the anti-freezing design requirements for water system pipelines, the system functions in cold regions should be tested firstly. The common methods for predicting environmental temperature include CFD simulation calculations and Analytical calculation method [5-7], Zhang Teng et al. [8] conducted temperature measurements in open, semi-open, and enclosed structural compartments for one year, and the results showed that the temperature data at all measurement points was basically the same at night, with a maximum temperature difference within 3 °C. Therefore, in engineering

Y. Zhang et al. (eds.), *Proceedings of the 2024 10th International Conference on Architectural, Civil and Hydraulic Engineering (ICACHE 2024)*, Advances in Engineering Research 259,
https://doi.org/10.2991/978-94-6463-658-1_84

application, when an aircraft was parked in a cold area during nighttime enough long, it could be considered that the temperature differences between the aircraft compartments could be ignored.

When operating in cold regions, the water system should be filled after the aircraft starts and air conditioning system works. As the aircraft starts, each compartment responses differently in temperature due to its sealing status, heat from equipment/pipelines and insulation structures. According to the temperature data obtained from the sensors near the water system pipelines of a certain type of aircraft during the initial stage of air conditioning system start-up (within 30 minutes) after a long stay in extremely cold regions, the external environment of the pipelines was divided into two categories: semi-open compartments and enclosed compartments. The ambient temperature was shown in Table 1.

Table 1. Ambient temperature in the different compartments

Areas	Temperature (°C)
Enclosed compartments	-5.5±1.0
Semi-open compartments	-10.8±0.4

2 Anti-freezing Design in the Different Compartments

2.1 Geometric Model and Material Properties

The water system pipelines mainly consist of pipe walls and two end joints, with an inner diameter of 12.7 mm. The pipe wall is made of rubber and has a thickness of 4mm. Since the length is usually far larger than inner diameter, the heat transfer of the pipelines could be simplified as a one-dimensional heat transfer issue. The physical properties of pipeline materials and fluid medium were shown in Table 2.

Table 2. Material properties

Materials	Density (kg/m^3)	Thermal conductivity (W/(m*°C))	Specific heat capacity (J/(kg*°C))
water	-5.5±1.0	0.58	4200
rubber	-10.8±0.4	0.27	1700

2.2 Heat Transfer Equations

The analysis of the operational scenarios of the water system showed that when water filled before the flight, the zero flow state of the pipelines was the most severe condition. The water flow in the pipelines dissipated heat into the compartments through the wall of the pipelines. While the water temperature inside the pipeline decreased, the heat transfer also gradually decreased. This process is a non-steady heat transfer process.

For the convenience of calculation, the following assumptions were made:

1) The temperature of the water flow was the same as the temperature of the inner wall of the pipeline;

2) When the time element dt is small enough, it is considered that the wall temperature of the tube remains constant during this time period, and the wall temperature in the next element varied.

According to heat transfer theory [9], the heat loss of water flow through the pipe wall during the dt time was shown in formula (1) and the water temperature decreased as shown in formula (2):

$$Q^n = \frac{2\pi L(T_f^{\ n} - T_\infty)}{\left(\ln d_0 / d_i\right)/\lambda + 2L/hd_0} dt \quad (1)$$

$$T_f^{n+1} = T_f^n - \frac{Q^n}{c_p m} \quad (2)$$

Wherein

d_0 -inner diameter of pipelines, m;

d_i-outside diameter of pipelines, m;

T_f-temperature of inner wall of pipelines, °C;

T_∞-environmental temperature, °C;

λ- thermal conductivity, W/(m·K);

h- heat transfer coefficient, W/(m^2·K);

c_p-specific heat capacity, J/ (kg·K).

Because water temperature inside the pipelines was low, the radiation could be neglected. The heat loss mainly included the heat transferred to the compartments. For a typical pipeline model, the calculation for convective heat transfer coefficient was as follows in formula (3)- formula (5):

$$h_f = \frac{Nu}{d_0}\lambda \quad (3)$$

$$N_u = 0.36 + 0.363 Gr^{1/6} + 0.0914 Gr^{1/3} \quad (4)$$

$$Gr = \frac{g\alpha d_0^3 \left(T_w - T_\infty\right)}{\upsilon^2} \quad (5)$$

Wherein,

d_0 -inner diameter of pipelines, m;

T_w-temperature of outside wall of pipelines, °C;

T_∞-environmental temperature, °C;

λ- thermal conductivity, W/(m·K);

g- heat transfer coefficient, m/s^2;

υ - dynamic viscosity of air, m^2/s.

2.3 Heat Transfer Equations with Inner Heat Source

After adding electric heat tracing, it was necessary to calculate the temperature distribution inside the pipelines to verify the effectiveness of electric heat tracing. The non-steady heat transfer process with an internal heat source satisfies the following formula (6). Due to the symmetrical distribution of temperature along the radius inside the pipelines, the temperature at points on the same circumference was equal. Therefore, formula (6) could be transformed into a two-dimensional problem with (r, z) coordinates, as shown in formula (7).

$$\rho c\frac{\partial t}{\partial \tau}=\frac{\partial}{\partial x}\left(\lambda\frac{\partial t}{\partial x}\right)+\frac{\partial}{\partial y}\left(\lambda\frac{\partial t}{\partial y}\right)+\frac{\partial}{\partial z}\left(\lambda\frac{\partial t}{\partial z}\right)+\Phi \tag{6}$$

$$\rho c\frac{\partial t}{\partial \tau}-\frac{1}{r}\frac{\partial}{\partial r}\left(\lambda r\frac{\partial t}{\partial \tau}\right)-\frac{\partial}{\partial z}\left(\lambda\frac{\partial t}{\partial z}\right)=\Phi \tag{7}$$

Wherein,
ρ−density, kg/m^3
c-specific heat capacity, J/ (kg·K).
λ- thermal conductivity, W/(m·K);
Φ-inner heat source, W/m^3;
r- radius, m.

MATLAB PDE-tool provides a powerful and flexible environment for solving two-dimensional finite element partial differential equations [10]. The boundary conditions should set as following:

1) The left and right boundaries of the analysis domain, representing the two ends of the pipelines, and the upper boundary of the analysis domain, representing the outside wall of the pipelines, were all the Newman boundaries. The convective heat transfer coefficients of the pipelines in enclosed and semi-open compartments were the same as before;

2) The lower boundary of the analysis domain is the center of the pipeline, and the heat flux density on this boundary was 0.

3 Results and Discussion

3.1 Heat Loss in the Different Compartments

Taking a one-meter-long pipeline as an example, the heat loss and temperature varying with time in semi-open and enclosed compartments were studied, as shown in Fig. 1.

According to Fig. 1, the water temperature in the pipelines gradually decreased with time, while the cooling rate gradually decreased. The heat loss of the pipelines gradually increased with time, while the rate of increase gradually slowed down. Because of lower ambient temperature and stronger heat transfer effectiveness in semi-open compartments, the pipelines water temperature dropped significantly faster than that in enclosed compartments at the same temperature, and the rate of heat loss in semi-open compartments is significantly higher than that in enclosed compartments. When the filled water temperature was 25°C, in enclosed compartments, the water temperature decreased to 0°C after about 1500s, and then the water temperature was no longer reduced with liberating the latent heat of condensation. Within half an hour before flight, the water in the pipelines would not freeze; In the semi-open compartment, the water temperature decreased to 0°C after about 750s, and then changed similar to that in enclosed compartments. Within half an hour before the flight, the water in the pipeline would not freeze.

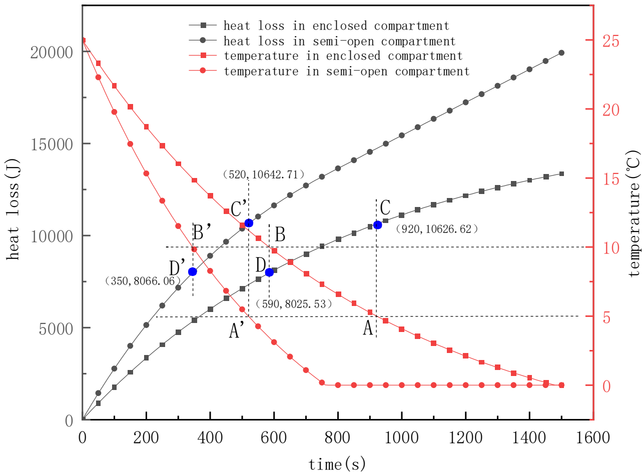

Fig. 1. The graph of temperature and heat loss variation with time

To ensure that water temperature would not drop to excessively low during long-term service before flight, the target temperature for the pipelines was usually set at around (6±2) °C. When the water temperature dropped to 6 °C, if the electric heat tracing supplemented the heat equivalent to the heat loss, the water temperature would not continue to decrease. In order to maintain the water temperature, the average heat loss power within the range of 5 °C -10 °C was used as the design power for electric heat tracing. According to the Fig. 1, the time points of water temperature at 5 °C and 10 °C in enclosed compartments and semi-open compartments could be captured, that is, the x-coordinates of points A and B, and the x-coordinates of points A 'and B'. The heat loss during this time interval could be captured, that is, the y-coordinate of points C and D, and the y-coordinate of points C 'and D'.

Therefore, for 12.7 mm-diameter pipelines in enclosed and semi-open compartments, the recommended powers of the electric heat tracing were shown in Table 3.

Table 3. Recommended powers of the electric heat tracing

Areas	Powers of the electric heat tracing (W/m)
Enclosed compartments	9.50
Semi-open compartments	18.20

3.2 The Temperature Distribution of Pipelines with Electric Heat Tracing

After adding the electric heat tracing according to Table 3, the temperature distributions inside the pipelines were shown in the Fig. 2 and Fig. 3. Due to convective heat transfer, there was a significant temperature gradient between the left and right sides of the pipeline, as well as the pipeline wall, and the pipelines water temperature.

Assuming the initial temperature of the water inside the pipelines was 10 °C, in enclosed compartments, after 1800s, the water temperature in the core area was about 5.6 °C, while that of the pipe wall was about 4 °C. After 3600s, the water temperature in the core area rose to 6 °C, while that of the pipe wall was about 4 °C. After 7200s, the temperature stayed equally to that at 3600s, indicating that after an hour, the temperature distribution in the pipelines was basically stable, with a water temperature of about 6 °C which was within target temperature.

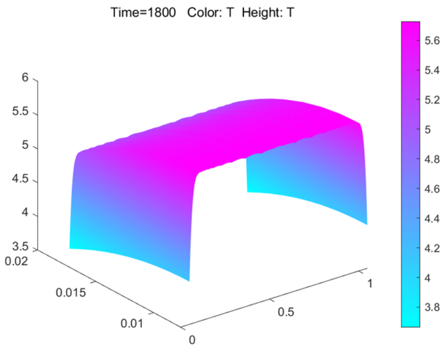

(a) at 1800 s

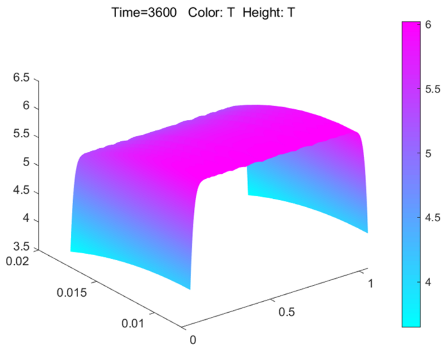

(b) at 3600 s

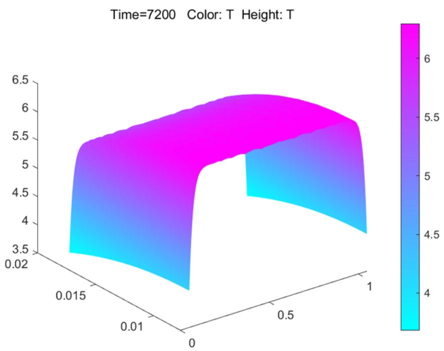

(c) at 7200 s

Fig. 2. Temperature distribution of pipelines in enclosed compartments

In semi-open compartments, after 1800s, the water temperature in the core area was about 6 °C, while that of the pipe wall was about 4 °C. After 3600s, the water temperature in the core area rose to 6.5 °C, while that of the pipe wall was about 4 °C. After

7200s, the water temperature in the core area rose to 7 °C, while that of the pipe wall was about 4.5 °C. In 2 hours, in the semi-open compartment, the water temperature in the pipelines was 6 °C -7 °C, within the target temperature.

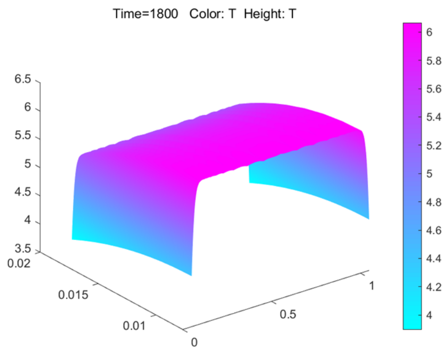

(a) at 1800 s

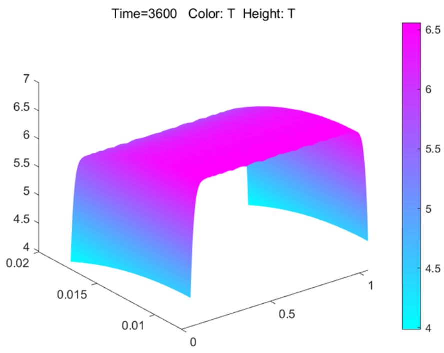

(b) at 3600 s

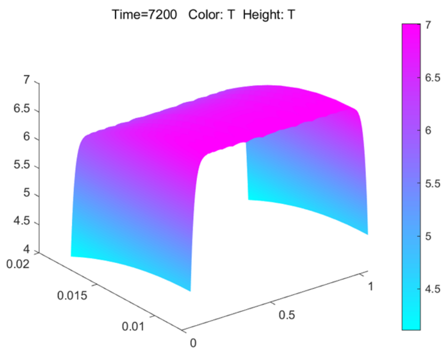

(c) at 7200 s

Fig. 3. Temperature distribution of pipelines in semi-open compartments

4 Conclusion

The water temperature and heat loss of the pipelines in enclosed and semi-open compartments varied with time similarly. The water temperature decreased with time, and the rate of decrease gradually slowed down; The heat loss increased with time, and the rate of increase gradually slowed down. Because of the lower ambient temperature and stronger heat transfer effectiveness, the water temperature in the semi- open compartments dropped faster and the heat loss was greater.

MATLAB PDE-tool can solve two-dimensional differential equations containing internal heat sources, which could display the temperature distribution inside the pipelines at different time points.

Using the average heat loss power within the range of 5 °C-10 °C as the design power for electric heating, the water temperature could be maintained at the target temperature of (6±2) °C within 2 hours.

References

1. Lei Meiling. (2012) Research on types of water system for new civil aircraft[J]. Advances in Aeronautical Science and Engineering, 3(2):229-234.
2. Xiao Jia, Yang Bo, Wang Yunlu. (2012) Modeling and simulation of water system under framework of electromechanical integrated management [J]. Computer Engineering and Design, 33(5):1943-1947, 1972.
3. Zhou Fei. (2015) Brief introduction of winter maintenance characteristics of Boeing 737NG. Science and Technology, 18:159.
4. Geng Yu. (2020) Selection of Heat Tracing Technology in Pipeline Anti-freezing Design Scheme. Engineering and Technology, 47:114-116.
5. Zhao Xuan. (2016) Numerical simulation of aircraft skin temperature field and local icing process[D], Harbin Institute of Technology.
6. Earl AT, Ken Morgan. Application of Integrate Fluid-Thermal-Structural Analysis Methods [R]. IC AS-88-233.
7. Zhang Bei. (2014) Natural Convection Heat Transfer Study and Thermal Analysis within an Aircraft Complex Enclosed Space[D], Harbin Institute of Technology.
8. Zhang Teng, He Yuting, Li Changfan, Zhang Haiwei, Houbo. (2015) Research on local temperature environment of ground parking aircraft [J]. Acta Aeronautica et Astronautica Sinica, 36: 538-547.
9. Tao Wenquan. (2019) Heat Transfer (fifth edition). Higher Education Press, Beijing.
10. Xiong Jing, Zhang Wei. (2009) Applications of PDE-tool of Matlab to heat conduction [J]. Industrial Heating, 38: 42-44.